Molecular Rheology of Comb Polymer Melts. 1. Linear Viscoelastic Response

D. R. Daniels,*,† T. C. B. McLeish,† B. J. Crosby,† R. N. Young,‡ and C. M. Fernyhough‡

IRC in Polymer Science and Technology, Department of Physics and Astronomy, University of Leeds, Leeds, LS2 9JT, UK, and Department of Chemistry, University of Sheffield, Sheffield, S2 2UN, UK

Received April 25, 2001; Revised Manuscript Received July 17, 2001

ABSTRACT: We present experiments and theory on the melt dynamics of monodisperse entangled polymers of comb-shaped architecture. Frequency-dependent rheological data on a series of comb polymers are in good agreement with a tube-model theory that combines star polymer melt behavior at high frequency with modified linear polymer reptation behavior at low frequencies. Taking into account mild polydispersity and by incorporating the high-frequency Rouse modes, we are able to model quantitatively the entire frequency range. Qualitatively distinct dynamical features of the comb architecture are compared to those of the simpler star and H-topologies.

1. Introduction

The observed complex rheological properties of polymer melts are well described by the tube model of entanglements.[1] It predicts very different entangled dynamics for the cases of linear[2,3] and star-shaped[2,3] chains. Linear chains renew their configurations via a process known as reptation, which gives rise to a dominant characteristic relaxation time scale, τ_{rep}. Star polymers, on the other hand, must rely on a type of "activated diffusion", arising from breathing motions of the arms, to renew chain configurations ever closer to their branch points. This leads to a very broad spectrum of relaxation times, with the longest relaxation time having an exponential dependence on the arm molecular weight.[4]

Tube inspired models have now become increasingly advanced[5] and have recently been applied to more complex architectures, e.g., the H-architecture.[6] H-polymers possess four starlike arms connected by a central "cross-bar" and combine the features of star and linear polymers in linear response in new and novel ways. Typically[7,8] the cross-bar provides reptation-like relaxations at lower frequencies while the arms provide starlike relaxations at higher frequencies, consistent with a separation of time scales into fast (arms) and slow (cross-bar) times.[9,10] For more details the reader is referred to ref 6.

The success of the tube model in the H-polymer case motivates this study of comb-shaped polymer melts, the next case in a series of increasingly complex topologies. Comb polymers possess a number of starlike arms distributed along a central backbone, unlike H or pom-pom polymers where the arms are concentrated at the backbone end points. Some viscoelastic data on lightly entangled comb polystyrenes exist,[8] and a rudimentary application of the tube model suggested a similar time scale separation of relaxation times for arm and backbone as in H-polymers.[11] For comb polymers the arms continue to provide starlike excitations at higher frequencies with the backbone providing reptation-like relaxations at lower frequencies. Because of the distribution of arms along the comb cross-bar, however, this opens up an additional spectrum of relaxations at lower frequencies for comb polymers, not available to H or pom-pom polymers. This property of comb polymers produces novel and significantly different linear rheological response at lower frequencies in comb polymers compared to H or pom-pom polymers. Very recently, a polyisoprene comb with eight arms on an entangled backbone was reported to exhibit anomalously low viscosity and terminal relaxation time (lower even than a pom-pom polymer of similar arm fraction and identical molecular weight, but with half the cross-bar molecular weight). This was conjectured to be due to additional Rouse-like relaxations available to combs. Our extensive series of comb architectures would be hoped to shed light on such a surprising result.[13]

Recent developments in tube theory of branched polymers have motivated the synthesis of a series of polybutadiene combs, highly entangled and of variable architecture; this is the subject of an accompanying paper to this one.[14] They are the subject of the rheology and theory of this study. The materials of our study also introduce a limited degree of stochastic variation in molecular topology. Although the molecular weights of cross-bar and arms are monodisperse, the method of attachment of arms to the cross-bar[14] yields a Poisson distribution in the number of attached arms.

Below, we will find for comb polymers two distinct and discernible regimes for the low-frequency relaxations. If the number of arms distributed along the crossbar is relatively small, then we find that the comb backbone behaves essentially as a H-polymer crossbar.[6] On the other hand, if the number of arms along the comb crossbar is relatively large, then we find the low-frequency relaxations to be drastically altered, and the linear rheological response of comb polymers will differ markedly from that of H-polymers.

In the next section we describe the synthesis and experimental rheology. In following sections we derive the tube-model theory for well-entangled comb polymers in linear step strain. We then conclude in the final section with a discussion of results obtained. A number

† University of Leeds.
‡ University of Sheffield.

10.1021/ma010712p CCC: $20.00
Published on Web 08/30/2001

Table 1. Comparison of Theory (fit) and Chemistry (ch) Parameters for Comb Polymers Studied

polymer	s_a(ch)	s_a(fit)	s_b(ch)	$s_b(\mathrm{fit})_R$	ϵ_a(ch)	ϵ_a(fit)	ϵ_b(ch)	ϵ_b(fit)	q(ch)	q(fit)
PBC2	10.3	12.8	123.2	124.3	1.02	1.05	1.02	1.05	31.6	22
PBC3	17.7	16.8	124.6	111.6	1.01	1.02	1.06	1.01	4.9	5
PBC4	24.6	26.8	120.1	149.2	1.07	1.08	1.03	1.10	25.2	20
PBC5	11.9	12.4	63.9	68.7	1.04	1.06	1.06	1.01	8.6	8
PBC6	28.8	25.3	60.5	72.9	1.03	1.04	1.03	1.01	9	8
PBC7	22.7	23.1	61.4	74.1	1.07	1.07	1.03	1.01	8.4	8
PBC8	22.7	26.1	118.5	127.1	1.00	1.02	1.02	1.13	3.4	5
PBC9	20.1	20.9	81.8	87.6	1.00	1.03	1.00	1.02	7.7	8
PBC10	14.9	14.4	53.8	64.7	1.00	1.02	1.00	1.01	8.0	7
PBC11	5.8	6.3	62.7	64.0	1.03	1.04	1.03	1.02	8.2	7

of further details of the background theory can be found in refs 5 and 6.

2. Experiment

2.1. Synthesis. Butadiene was polymerized in *n*-hexane using *sec*-BuLi as the initiator in an all-glass apparatus flamed under vacuum before use at 30 °C using normal anionic synthesis techniques.[14] NMR analysis revealed that the degree of 1,2 addition of butadiene was 7%. ClMe2HSi was used to functionalize a fraction of these dangling vinyl moieties on a linear PB "backbone" for the comb architecture via a catalyzed hydrosilylation. The "branches" of the comb were attached by preparing PB−Li linear fraction in a manner similar to the backbone. The "branches" then reacted (nucleophilic) at the Si−Cl functional sites on the "backbone". Samples were taken for subsequent analysis prior to reacting "branches" with "backbone". Capping of the functionalized vinyl groups was achieved by adding *n*-BuLi after 24 h.[14] This procedure is expected to yield Poisson distributions of the number, q, of attached arms to the monodisperse backbones.[14] The comb product and linear constituents were measured in a GPC with L/M-ALLS detection to measure architectural parameters such as "branch" M_w, "backbone" M_w, polydispersity (M_w/M_n), and branches per backbone. In Table 1 we can see that 10 comb polymers were used in this study, with varying number of entanglements along the backbone s_b and along the arms s_a and number of arms q. For example (see Table 1), PBC2 and PBC4 each possess a relatively large number of arms, with PBC4 having an arm length roughly twice that of PBC2. PBC3 and PBC8 possess relatively few arms, with almost equal backbone lengths, while PBC8 possesses slightly longer arms. The remaining comb polymers used each contain a similar number of arms and similar backbone lengths (apart from PBC9 which has a backbone some $^1/_3$ greater). The main difference in the remaining comb samples lies in their arm lengths. For example, PBC11 has relatively short arms, whereas PBC6 has much longer arms (see Table 1).

2.2. Rheology. For rheology, the samples were pressed either in nitrogen or in vacuo into 10 mm diameter disks. These samples were compressed between the opposing fixtures in the rheometer until the desired gap was achieved. For linear rheology 10 mm parallel plates with between 0.8 and 1.2 mm gaps were chosen. The samples were loaded and trimmed at room temperature followed by further compressing by about 10%. Rheometrics Scientific Incorporated (RSI) RDA 2 or RDS2 rheometers were used to measure rheological parameters. Dynamic frequency sweeps were performed such that the upper frequency was 100 rad/s, and the lower band was between 0.1 and 10−3 rad/s in the linear strain regime (as determined by overlaying with similar sweeps but with strains different by a factor of 2). Temperatures were between 100 and −90 °C with nitrogen purge. The highest temperatures were only attempted after completion of low-temperature work was finished. Overlaying of room-temperature rheograms was done to check for sample degradation, of which there was none. RSI Orchestrator software was used to perform time−temperature superposition of data taken at different temperatures and to produce master curves. The overlay technique selected was first frequency (horizontal) shifting to minimize tan(δ) residuals followed by vertical shifting to minimize residuals of viscoelastic moduli. In this way smooth master curves were obtained for all the polybutadiene samples. The vertical shifting was required to accommodate the thermal expansion of the plates at different temperatures.

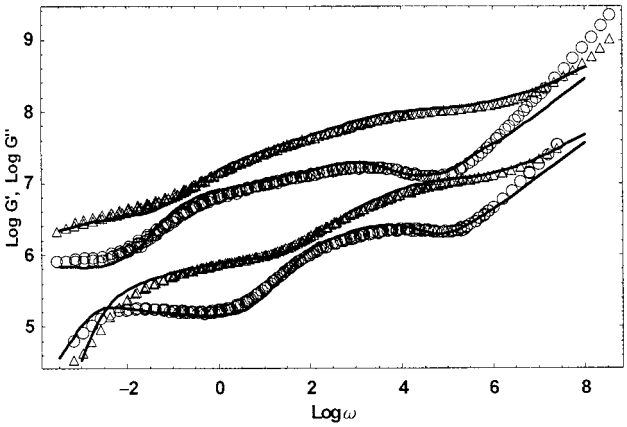

Figure 1. Comparison of high q experimental data and theoretical predictions for $G'(\omega)$ and $G''(\omega)$ for (from bottom to top) PBC2 and PBC4. Note the relatively low values of "backbone modulus" in these cases. PBC4 has been shifted vertically by a factor of 100.

2.3. Linear Rheology. The time-dependent modulus is calculated as a sum of contributions from the arms (or starlike part), the backbone (or linearlike part), and the high-frequency Rouse contributions. The dynamic modulus $G^*(\omega)$ is related by Fourier transform to the time-dependent modulus as $G^*(\omega) = i\omega\mathcal{F}[G(t)](\omega)$.[1]

Linear rheological spectra are given in Figures 1−4 for the polymers studied, together with the results of the theory developed below for each case. Overall, we see the obvious rheological "signatures" we expect from entangled comb-shaped structures. This is particularly clear in the shape of the $G''(\omega)$ curves. Free Rouse modes within the tube at high frequencies give $G''(\omega) \sim \omega^{1/2}$, progressing to lower frequencies where there is a minimum at $\omega < \tau_e^{-1}$, when entangled modes set in. This is followed by an extended "shoulder" feature whose width grows approximately linearly (on a log ω plot) with the molecular weight of the arms, M_a (see Figure 3). It corresponds to their relaxation by activated arm retraction. Finally, there is a weak maximum or step at lower frequencies coming from the relaxation of the cross-bars or linear portion. For comb polymers, the more highly entangled the cross-bars are with themselves the more sharply defined is their reptation peak.

Increasing the backbone molecular weight (Figure 4), M_b, takes the peak to lower frequencies, while reducing it both speeds up the cross-bar relaxation and weakens the magnitude of the peak as the volume fraction of backbone material, ϕ_b, reduces and with it its contribution to the modulus (as $\phi_b^{1+\alpha}$, where $\alpha = {}^4/_3$). So the comb polymer spectrum we expect contains features reminiscent of the spectra of both star (a broad shoulder in $G''(\omega)$) and linear polymers (a well-defined peak in $G''(\omega)$) at the frequencies corresponding to the inverse relaxation time of the structural components that resemble them (arms and cross-bar, respectively).

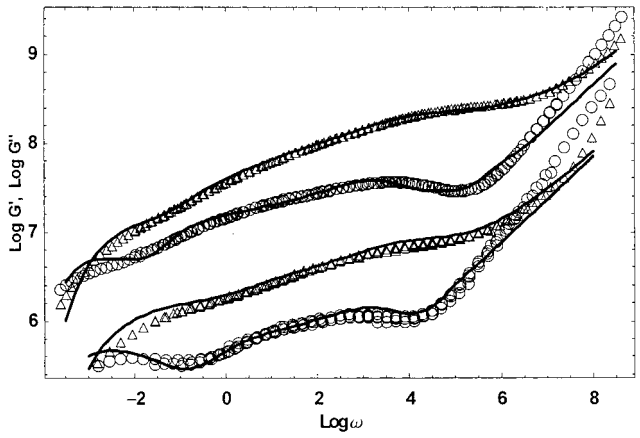

Figure 2. Comparison of low q experimental data and theoretical predictions for $G'(\omega)$ and $G''(\omega)$ for (from bottom to top) PBC3 and PBC8. Note the relatively high values of "backbone modulus" in these cases. PBC8 has been shifted vertically by a factor of 100.

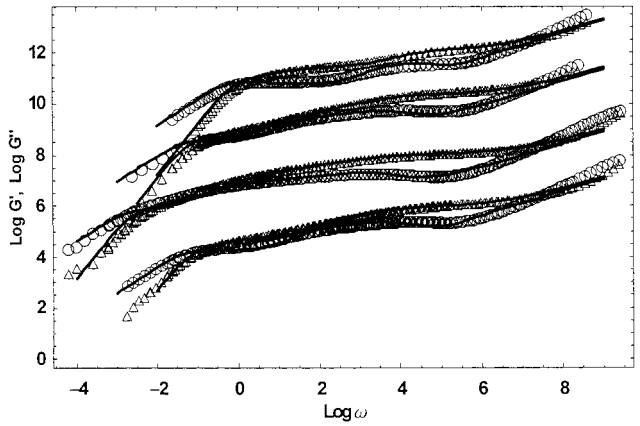

Figure 3. Comparison of experimental data and theoretical predictions for $G'(\omega)$ and $G''(\omega)$ for (from bottom to top) PBC5, PBC6, PBC10, and PBC11 comparing comb polymers with differing arm lengths. PBC6, PBC10, and PBC11 have been shifted vertically by factors of 10^2, 10^4, and 10^6, respectively.

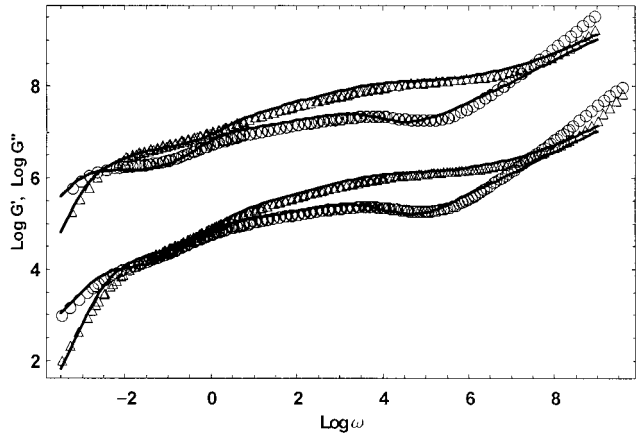

Figure 4. Comparison of experimental data and theoretical predictions for $G'(\omega)$ and $G''(\omega)$ for (from bottom to top) PBC7 and PBC9 comparing comb polymers with differing backbone lengths. PBC9 has been shifted vertically by a factor of 100.

3. Linear Response and Relaxation Times

We now proceed to outline the theory used and relevant time scales[5,6] for comb polymers.

At early times stress will relax in any dangling arms by rapid Rouse motion of the chain end along its tube, just as for star polymers[4] except for the presence of effectively "frozen" backbone material. At later times, this rapid path length fluctuation crosses over to an exponentially slow "activated diffusion" for the deeper arm fluctuations. The effective tube diameter grows continuously and self-consistently throughout this regime, and the comb cross-bar remains effectively immobile. After the starlike arms have completely retracted, we need to consider the mobility of the cross-bars present in widened tubes defined only by their mutual entanglements. The effective friction in the case of comb polymers with relaxed dangling arms is concentrated along the backbone at the branch points. This contrasts with the case for H-polymers, where all the friction is concentrated at the crossbar end points. But just as with H-polymers, the rapidly fluctuating arms provide drag that far outweighs the sum of monomeric drags along the cross-bars. This means that the total drag on the backbone will vary as the number of side branches q, not as M_b. Initially, stress is lost from cross-bar segments via uncorrelated diffusion of the branch points along the tube (analogous to the early motion of the free arm ends). The diffusion of the chain ends is suppressed when path length fluctuations become slowed by the effective elastic potential (so thinking of the cross-bar as a "two-arm star"[15]). Central portions of the cross-bar are relaxed by reptation. This is the slowest contribution to the linear stress relaxation.

Following ref 6, the key ingredients required for our model are as follows. We need to calculate a hierarchy of time scales $\tau(x)$ in terms of an arc length coordinate x that runs from the ends of a polymer chain to the center. For example, in star polymer melts, x takes the value 0 at the chain ends and increases to 1 at the core where the arms meet. We must also write a form for the effective modulus of an entanglement network corresponding to a concentration $\Phi(x)$, where $G(\Phi) = G_0\Phi^{1+\alpha}$ and $\Phi(x)$ is the concentration of unrelaxed material when segments with coordinate x are just relaxing (i.e., at the time scale when tube segments at x are just being reached by free ends for the first time). These are the assumptions of the "dynamic dilution" hypothesis. Then an expression for the relaxation modulus $G(t)$ may be written from the general expression[5,15]

$$G(t) = \int_0^1 \frac{\partial G(\Phi(x))}{\partial x} e^{-t/\tau(x)}\, dx \qquad (1)$$

This expression assumes only that the effective modulus at time t depends on the amount of unrelaxed tube and is valid providing all currently unrelaxed chain has been able to explore fully the dilated tube at t. At time t the unrelaxed fraction of chain is $\Phi(x(t))$.

For comb polymers it is natural to divide the arc coordinate into two sections: x_a runs along the arms from the ends to the branch points ($0 < x_a < 1$), and x_b runs from the branch point to the middle of the cross-bar ($0 < x_b < 1$). Now (1) becomes

$$G(t) = G_0(\alpha+1)\left\{\int_0^1 \phi_b^{\alpha+1}(1-x_b)^\alpha e^{-t/\tau_b(x_b)}\, dx_b + \int_0^1 (1-\phi_a x_a)^\alpha \phi_a e^{-t/\tau_a(x_a)}\, dx_a\right\} \qquad (2)$$

Here ϕ_a and ϕ_b are the volume fractions of arms and cross-bar, respectively. The first term comes from the contribution of cross-bar material and the second from

the relaxation of the dangling arms. In each integral, the term in round brackets represents physically the effective concentration of unrelaxed entangling network surrounding a segment relaxing on a time scale $\tau_{a/b}(x)$. We now turn to the derivation of the relaxation time scales for the dangling arms $\tau_a(x)$ and for the cross-bar $\tau_b(x)$ (see also ref 6).

3.1. Arm Relaxation. The very outermost tube segments are relaxed by curvilinear Rouse motion of the free end and has a spatial mean displacement s following the sub-Fickian form $s \sim t^{1/4}$. Inversion and substitution of the Rouse result in terms of monomeric friction provides a characteristic time for the diffusion of free ends to segments at arc coordinate x:[5]

$$\tau_{early}(x) = \frac{225\pi^3}{256}\left(\frac{N_a}{N_e}\right)^2 \tau_R x^4 \tag{3}$$

in terms of the Rouse time τ_R of the dangling arm.

Note that the use of this expression as an effective first passage time involves two approximations: that of single-exponential relaxation of stress per segment and the equivalence of first passage time to inversion of the mean displacement of the chain end, $\langle r^2(t)\rangle$. Simulations indicate that neither is exact but that the use of such expressions yield good approximations for $G(t)$,[16] and exact calculations are underway[16] for future comparison.

Beyond an arc coordinate $x \sim (M_a/M_e)^{-1/2}$ fluctuations of the entangled path length of the arm begin to require entropically unfavorable unentangled folded loops either within the tube or emerging from its sides. The elastic potential for such retractions in a fixed network was calculated by Pearson and Helfand[17] to be $U_0(x) = kT\nu s_a x^2$ with the constant $\nu = 15/8$ and $s_a = M_a/M_e$. However, as we have seen, the tube diameter relevant to further retractions at any time scale is diluted by all material occupying tube segments already relaxed. This leads to a renormalization of the potential to an effective potential $U_{eff}(x)$ which takes into account the dilution of the entanglement molecular weight as a function of relaxed material fraction $M_e(x)$.[18] This can be achieved self-consistently, and $U_{eff}(x)$ is generally given in terms of the solution of the differential equation

$$\frac{dU_{eff}}{dx} = \frac{\partial U_0(x;M_a,M_e(x))}{\partial x} \tag{4}$$

which says that the effective dilution of the potential from segments at x may only be realized for processes on time scales $\tau(x)$ or longer.[17]

An approximation for the mean first-passage time for diffusers over such a potential barrier as $U_{eff}(x)$ can be calculated analytically for all x in terms of integrals over the potential (see ref 6).

$$\tau_{al}(x_a) = \frac{L_a^2}{D_{a,eff}} \frac{\exp[U_{a,eff}(x_a)]}{U'_{a,eff}(x_a)}\left(\frac{\pi}{2U''_{a,eff}(x_a=0)}\right)^{1/2} \tag{5}$$

where $L_a^2/D_{a,eff} = 15\pi^2 s_a \tau_R/8$. By crossing over smoothly to eq 3 for small x, the spectrum of arm relaxation times $\tau_a(x)$ is calculated, including a weakly x-dependent prefactor.[6]

$$\tau_a(x_a) = \frac{\tau_{ae}(x_a)\exp[U_{a,eff}(x_a)]}{1 + \tau_{ae}(x_a)\exp[U_{a,eff}(x_a)]/\tau_{al}(x_a)} \tag{6}$$

This simple crossover form works because $\tau_a(x_a)$ goes as $\tau_{ae}(x_a)$ for small x_a when $U_{a,eff}(x_a)$ and $\tau_{ae}(x_a)/\tau_{al}(x_a)$ goes to zero. Similarly, $\tau_a(x_a)$ goes as $\tau_{al}(x_a)$ as $\tau_{ae}(x_a)\exp[U_{a,eff}(x_a)]/\tau_{al}(x_a) \gg 1$ for intermediate values of x_a.

The application of this procedure, as outlined, to the activated retractions of star and H-polymer arms is discussed in ref 6, where the form of the effective potential is given as

$$U_{a,eff}(x_a) = \frac{15s_a}{4}\frac{1-(1-\phi_a x_a)^{\alpha+1}(1+(1+\alpha)\phi_a x_a)}{(1+\alpha)(2+\alpha)\phi_a^2} \tag{7}$$

It is easy to see that the potential well is deeper and steeper than for pure star polymers, due to the fraction of cross-bar material that behaves as permanent network for the relaxing arms. In this way for H and comb polymers, the fraction of arm material enters into the exponent for the longest relaxation time among arm retractions, which becomes (the version of eq 5 applicable to comb polymers)

$$\tau_a[1] \sim \exp\left[\frac{15s_a}{4}\frac{1-(1-\phi_a)^{\alpha+1}(1+(1+\alpha)\phi_a)}{(1+\alpha)(2+\alpha)\phi_a^2}\right] \tag{8}$$

We notice one very important physical consequence of the cooperative nature of the arm relaxations: the longest relaxation time of the arms is exponentially dependent not only on the number of entanglements on each arm s_a but also on the arm fraction ϕ_a. Increasing the amount of material in the cross-bars, which acts as a permanent network throughout the relaxation of the free arms, greatly extends the slowest mode of the arms. So star-arms attached to cross-bars of an H-polymer or comb polymer melt would be expected to exhibit exponentially slower relaxation times than when attached to simple branch points as in a melt of pure stars. This is the reason for Roover's early observation[7,8] that the "viscosity enhancement" of dangling arms (over the value they would have as linear polymers) was much greater in his comb and H-polystyrenes than in the corresponding stars. We expect to observe the same phenomenon in entangled combs, but more sensitively, since the arm fraction ϕ_a varies with M_a multiplied by the number of arms q, which may reach values as high as 30 in our samples.

3.2. Backbone Relaxation. Once the arms have relaxed the comb backbones behave as linear polymers, entangled with each other only, moving against drag concentrated at the branch points. Portions of tube are renewed first by fluctuation of the backbone path length and then by reptation of the remaining backbone as a whole. The form of the very earliest fluctuation-dominated relaxation depends on whether the number of arms is large or small, as we will find below, but at later times the activated fluctuation in all cases takes a form similar to the H-polymer case.[6] The spectrum of relaxation times may be constructed by thinking of linear polymers as "two-arm stars" for times less than their reptation time.

A crossover formula for the spectrum of relaxation times $\tau_b(x)$ is constructed in an analogous way to $\tau_a(x)$ above (for details see ref 6) such that

$$\tau_{b,ret}[x_b] = \frac{\tau_{be}[x_b]\exp[U_{b,eff}[x_b]]}{1 + \tau_{be}[x_b]\exp[U_{b,eff}[x_b]]/\tau_{bl}[x_b]} \tag{9}$$

where

$$\tau_{bl}(x_b) = \frac{{L_b}^2}{4D_{b,eff}} \frac{\exp[U_{b,eff}(x_b)]}{U'_{b,eff}(x_b)} \left(\frac{\pi}{2U''_{b,eff}(x_b=0)}\right)^{1/2} \quad (10)$$

is the late time activated result, with $D_{b,eff}$ calculated below, $U'_{b,eff}(x_b) = 15 s_b \phi_b{}^\alpha x_b(1 - x_b)^\alpha/8$ and $U''_{b,eff}(x_b=0) = 15 s_b \phi_b{}^\alpha/8$. We now consider the form of the relaxation times for the early and late time backbone fluctuation spectrum, in the two cases of small and large numbers of arms. The criterion for deciding between each case for a given sample is discussed in section 4.

3.3. Case 1 (Small Number of Arms). We expect comb polymers with a small number of arms to behave essentially as H-polymers, in that the early-time (unactivated) path length fluctuations are dominated by the diffusion of the terminal branch points alone. When the path length of the dangling arms eventually fluctuates to zero, corresponding to the free end retracing a path through the melt to the branch point itself, the branch point may make a diffusive hop through the melt. At this time scale of $\tau_a(1)$, the tube diameter is set only by other comb cross-bars so has a value $a^* = a\phi_b{}^{-\alpha/2}$. There is a slight uncertainty in the $O(1)$ number that relates the time scale of the hop to the mean hopping distance, so we will set the effective curvilinear diffusion constant of the branch point to the value[12]

$$D_{b,eff} = \frac{p^2 {a_{b,eff}}^2}{2\tau_a(1)} \quad (11)$$

where $p = 1/\sqrt{12}$, identical to the value chosen in ref 6 for H-polymers. (Note that p does not change with arm length, and in ref 6 the value of $p = 1/\sqrt{6}$ was erroneously reported.) Recently, it has been reported[19] that data on symmetric star polymers indicate that branch points hop in bare narrow tubes than in the "dilated" tubes considered here. However, for star polymers the diffusion of their branch points is a subtle consequence of the disentanglement transition, whereas our comb backbones remain entangled. We prefer to assume "dilated" tube hops here, leaving the physics of this question open to further examination.

The diffusive motion of the ends of the cross-bar is initially responsible for the loss of orientation and stress from its outer segments. In an analogy with the free Rouse diffusion orientation loss from the dangling arms, we write the "early form" for stress loss from the cross-bars as $\tau_{b,e} = x^2 L_{b,eff}{}^2/8D_{b,eff}$.[6] Note that the relaxation times depend on the cross-bar arc coordinate as x^2 rather than x^4 for the free ends. This is because the effective friction for motion of the branch points is concentrated at the branch points themselves—only a negligible correction comes from the true monomeric friction of the cross-bar chains themselves.

So (as outlined above and in ref 6), in the case where the early-time backbone fluctuation is dominated by the diffusion of a single branch point:

$$\tau_{be}[x_b] = \frac{25}{32p^2} s_b^2 \phi_b^{2\alpha} \tau_a[1] x_b^2 \quad (12)$$

is the early time relaxation result, near the cross-bar ends, with $L_{b,eff}/a_{b,eff} = {}^5/_4 s_b \phi_b{}^\alpha$.

A final crossover to the reptation time of the comb polymer cross-bars is also required, since their central sections will typically have starlike fluctuation times much longer than the center-of-mass reptation mode of stress–relaxation available to them. The reptation time for comb polymers with a small number of arms is determined by the time taken for the linear comb polymer cross-bar to diffuse the curvilinear length not already relaxed by fluctuations and so is given by the self-consistent relation

$$\tau_{rep} = \frac{25(1 - x_c)^2 {s_b}^2 \phi_b{}^{2\alpha} \tau_a[1] q}{4p^2\pi^2} \quad (13)$$

with $\tau_{bl}(x_c) = \tau_{rep}$, $\tau_d = (L_{b,eff}{}^2(1 - x_c)^2)/(\pi^2 D_{rep})$ and where a simple addition of drags from each branch point gives $D_{rep} = D_{b,eff}/q$.

3.4. Case 2 (Large Number of Arms). In the above analysis for a small number of arms it was assumed that the terminal frictional blobs, produced by an already relaxed arm attached at a branch point, acted independently from other frictional blobs. In this sense the motion of the comb backbone corresponded to the uncoupled dynamics of each separate frictional blob, and the center-of-mass diffusion constant for each blob dominated. For the case of many arms distributed along the comb cross-bar this physical picture is no longer valid, and we must now consider the coupled dynamics of all the frictional blobs taken together. In this limit the comb backbone behaves as an entangled Rouse chain with distributed drag. The Rouse expression for the mean displacement of the chain end is given by[1]

$$\langle \Delta R^2 \rangle = 2D_R \tau_R \sum_{n=1}^{q} \frac{1}{p^2} (1 - \exp(-n^2 \tau_{be}/\tau_R)) \quad (14)$$

where $\langle \Delta R^2 \rangle = (x_b L/2)^2$ is the average of the displacement squared and $D_R = D_{b,eff}/q$ and $\tau_R = 2L_{b,eff} a_{b,eff}/3\pi^2$ are the "renormalized" diffusion constant and Rouse time for the comb cross-bar. This is consistent with our modeling the cross-bar with frictional blobs distributed along its length as a "renormalized" Rouse chain. The effective friction, generated by the presence of already relaxed arm material at the branch points, vastly outweighs the monomeric friction and therefore becomes "renormalized" to a much higher value. The underlying physics remains the same, however.

In the high q limit, with again $L_{b,eff}/a_{b,eff} = {}^5/_4 s_b \phi_b{}^\alpha$, and converting the above sum into an integral over all n, we get

$$\tau_{be}[x_b] = \frac{375\pi}{4096p^2} q {s_b}^3 \phi_b{}^{3\alpha} \tau_a[1] x_b^4 \quad (15)$$

which corresponds to the case of highly coupled backbone frictional blob dynamics.

Again, we need a final crossover to the reptation time of the comb polymer cross-bars and so is again given by the self-consistent relation $\tau_{bl}(x_c) = \tau_{rep}$ with $\tau_d = (L_{b,eff}{}^2(1 - x_c)^2)/(\pi^2 D_R)$.

$$\tau_{rep} = \frac{375(1 - x_c)^2 {s_b}^3 \phi_b{}^{3\alpha} \tau_a[1] q}{256p^2\pi} \quad (16)$$

We can see by comparing the low and high q limits that the relaxation times for the case of high q are significantly increased with respect to the case of low q. This is due to the coupled nature of the frictional blob dynamics in the former case, as opposed to the un-

coupled nature of the frictional blob dynamics in the latter case. We will see how both of these separate dynamical scenarios for low and high q arise in the linear rheological response of different comb polymers below.

As stated in section 2.1, the number of arms follows a Poisson distribution. The main effect of this will be a contribution to the broadening of the "reptation peak" in $G''(\omega)$. (Other contributions such as constraint−release are not invoked at the current level of our theory.) This broadening will be directly proportional to the relative deviation in q, which is $1/\sqrt{q}$ for a Poisson distribution. We comment on the effect of this on our samples in the discussion below.

3.5. Rouse Modes ($\omega \geq 1/\tau_e$). For these high frequencies, the tube constraints do not significantly affect the relaxation modes of comb polymers, which proceed via Rouse dynamics on length scales smaller than a.

We write the Rouse spectrum for large frequencies as follows:[1]

$$G_R(t) = \frac{G_0 N_e}{N - N/N_e} \sum_{n=N/N_e}^{N} \exp(-n^2 t/\tau_R) \qquad (17)$$

where the Rouse time τ_R is given as $\tau_R = (N/N_e)^2\tau_e$ and τ_e is the entanglement time. Note that this expression for the Rouse spectrum differs slightly from the representation given in ref 20, although in reality this makes for little difference. Here we make the simpler assumption that Rouse modes are suppressed below the lowest limit in the above sum, so as to capture the crossover from entangled to pure Rouse behavior correctly. Rouse modes with a lower index are precisely those that are strongly affected by entanglement and relax via the sequence of retraction/activated retraction and reptation as discussed above. The normalizing prefactor is chosen such that $G_R(t=\tau_e) = G_0$. It is straightforward to calculate the contribution to response in frequency space by carrying out the appropriate Fourier transform.[1] Note that $G'(\omega) \sim G''(\omega) \sim \omega^{1/2}$ $\omega \rightarrow \infty$. For polybutadiene, however, it is routinely reported that the high ω behavior has a steeper slope than that predicted from the Rouse spectrum. This is almost certainly due to this regime being strongly affected by the α transition.

3.6. Polydispersity. Even though the materials investigated here were anionically polymerized, achieving the highest possible standards of monodispersity, we might expect that the exponential sensitivity of the branch point diffusion constant of the path length of the arms to amplify any slight polydispersity, especially in the molecular weights of the arms. Polydispersity induces two effects on the relaxation spectrum at times longer than $\tau_a(1)$: (i) a positive shift of the mean relaxation time; (ii) a spread of the relaxation times. In the comb polymer spectra, these may be particularly evident in the position and shape of the "reptation peak" at low frequencies. Calculations on arbitrary distributions via a moment analysis carried out in ref 6 tend to overestimate the effects of polydispersity on the average arm relaxation time. The treatment given in ref 6 assumed a fixed entanglement network, whereas the arm fraction of the entanglement network is mobile (with the backbone fraction fixed), and this will lead to some amount of "motional narrowing". Recent calculations that include the effect of motional narrowing have been carried out in ref 12, which involves solving the full Ball−Mcleish equation (4) in the presence of a distribution of polydisperse arms (see ref 12 for details).

Writing $M_w/M_n = 1 + \epsilon$, we find from ref 12 that to a good approximation small polydispersity effectively renormalizes the number of entanglements along an arm s_a to (with $\alpha = 1$):

$$s_{ar} \approx s_a + \frac{\nu_a s_a^2}{2}\epsilon_a \qquad (18)$$

where

$$\nu_a = \frac{15}{8}\frac{\phi_b^2}{\phi_a/3 + \phi_b} \qquad (19)$$

Thus, the polydispersity ϵ_a enters our expression for the arm relaxation time via its effect on s_a. (However, a change in the bare value of s_a can be distinguished from a change in ϵ_a since it is only s_a and not ϵ_a which has an effect on the concentration of arm material ϕ_a.)

An expression for the renormalized number of entanglements along the backbone s_b can also be constructed, where in this case the effects of motional narrowing are much smaller. The effects of polydispersity on the comb backbone dynamics is more subtle than the case for the motion of the comb arms, and in this case we use the treatment outlined in ref 6, which leads to a renormalized backbone length, s_{br}, of

$$s_{br} \approx s_b + \frac{\nu_b s_b^2}{2}\epsilon_b \qquad (20)$$

with

$$\nu_b = \frac{15}{8}\frac{\phi_b^{\alpha}(1 - (1 - s_d)^{1+\alpha}(1 + (1 + \alpha)s_d))}{(1 + \alpha)(2 + \alpha)} \qquad (21)$$

The spread in relaxation times increases rapidly with the molecular weight of the dangling arms, however, well-controlled the polydispersity. A similar effect arises in the contributions to the relaxation spectrum arising from the cross-bar because in practice a significant fraction of cross-bar material relaxes by fluctuation modes (see ref 6). Such a strong effect of polydispersity might have been expected in the simpler case of star polymers. However, in that case the mutual retraction dynamics proves to be strongly motion narrowing.[18] It is the presence of slowly relaxing cross-bar material that "amplifies" the inherent polydispersity of the arms' relaxation times. To appreciate more fully this high sensitivity to small polydispersity, more details on the determination of the polydispersity from chemistry and synthetic procedure will be given in an accompanying paper.[14]

4. Results and Discussion

Quantitative consideration requires careful comparison with curves calculated for $G^*(\omega)$ from the theory above. Polydispersity in the comb polymer case was treated at the relatively crude level of incorporating only the resulting shifts in the relaxation times. For comb polymers the polydispersity of the dangling arms is much more important than that of the cross-bars. Because of the slight uncertainties in molecular weight and polydispersities, the procedure adopted in each case for the comb polymers was to vary the values of M_a and

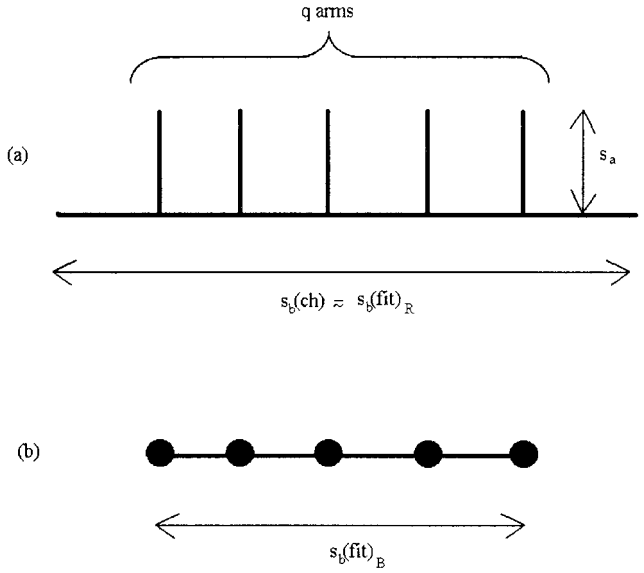

Figure 5. Diagram of a comb polymer illustrating the need for backbone length s_b correction.

M_b and polydispersities of arm and backbone via $\epsilon = M_w/M_n - 1$, until a fit with the data was obtained and then to check consistency with the results of other standard characterization methods reported above. The two universal (for PB) parameters G_0 and τ_e were also allowed minor adjustment within the range represented by rheology and experimental variation on samples with different synthesis but remained within factors of 1.2 of 1.25 MPa and 2.2×10^{-7} s at 25 °C. Values used for M_e were around 1850 g mol^{-1} for 1−4 PB, which we adhere to throughout. This is consistent with values of M_e quoted in refs 21 and 22, using the convention for M_e in which the appropriate coefficient for the activated diffusion potential is 15/8. Microstructure does have an effect on M_e, but in our case where we have PB 1−4, trans 54%, cis 40%, and vinyl 6%, an $M_e \sim 1900$ is correct,[21,22] while values of M_e between 1850 and 2000 have been quoted in ref 23. The value of τ_e used agrees well with the value given in ref 21, within a factor of 3, albeit given a slightly different microstructure. We found best-fit rheological values for the dimensionless structural parameters $s_a = M_a/M_e$, $s_b = M_b/M_e$, ϵ_a, and ϵ_b in each case. These are compared with the values obtained from synthesis and characterization in Table 1.

The theoretically predicted moduli $G'(\omega)$ and $G''(\omega)$ for PBC3 and PBC8 (shown in Figure 2) were calculated using the low q analysis outlined above, while $G'(\omega)$ and $G''(\omega)$ for the remaining samples were calculated using the high q analysis outlined above. All rheological data and model fitting at an effective temperature of 25 °C are give in Figures 1−4.

We have arranged the figures so that comparisons can be easily made of (i) high arm-number materials (Figure 1), (ii) low arm-number materials (Figure 2), (iii) effect of varying arm length (Figure 3), and (iv) effect of varying backbone length (Figure 4). Vertical shifts have been applied to each data set to separate them on the comparison plots.

To be able to make a comparison between the values of the backbone length derived from theory s_b(fit) and chemistry s_b(ch), we must proceed carefully due to the following (see Figure 5). Imagine following the portion of backbone from its end inward, toward the center until the very first branch point is reached. The "free end" portion of the backbone already traversed will contribute to the linear rheology in precisely the same manner as the other arms attached to the comb backbone. If this portion is shorter than M_a (as it will, on average, be if $M_b/(q+1) < M_a$), then the outermost branch points become mobile before arm retraction is complete. On the other hand, in all cases the length of the backbone is shorter than the original chemical length after arm retraction, since some of the backbone acts dynamically as arm material. We find that this phenomenon of "branch point evaporation" to affect the relatively low q PBC3 and PBC8 rather less than the other samples used, since for higher q the probability of hitting a branch point on the way in from the backbone end is markedly higher. To facilitate a realistic comparison of theory s_b(fit) and chemistry s_b(ch) for the comb polymers used, we need to incorporate this q dependence via an approximate correction to the backbone length s_b. Assuming the arms are distributed evenly along the backbone (monodisperse), we require the following mapping between the "renormalized R" and "bare B" values for s_b(fit) (see Figure 5):

$$\frac{s_b(\text{fit})_R}{s_b(\text{fit})_B} = \frac{1}{1 - \frac{2}{q+1}} \tag{22}$$

The values of s_b(fit) given in Table 1 are necessarily those of the corrected backbone length $s_b(\text{fit})_R$, which is the value that can be compared directly with the chemical value of the synthesized backbone s_b(ch). Note that $s_b(\text{fit})_R > s_b(\text{fit})_B$. Shown in Figure 6 is a comparison between $s_b(\text{ch})/s_b(\text{fit})_B$ (one data point for each material) and $s_b(\text{fit})_R/s_b(\text{fit})_B$ (dashed line), both plotted against the number of arms q. The value $s_b(\text{fit})_B$ corresponds to the backbone length relevant to rheological response, while $s_b(\text{fit})_R$ corresponds to the backbone length relevant to chemistry. We can see that our expression for $s_b(\text{fit})_R/s_b(\text{fit})_B$ (dashed line) accurately captures the observed behavior of $s_b(\text{ch})/s_b(\text{fit})_B$ (data points) for the comb polymers used over a wide range of values for the number of arms q. We emphasize again that $s_b(\text{fit})_R$ includes the comb terminal branches for direct comparison with the chemistry value s_b(ch), whereas the value $s_b(\text{fit})_B$ is used in the formulas such as (15) and (16) to calculate the low-frequency dynamics.

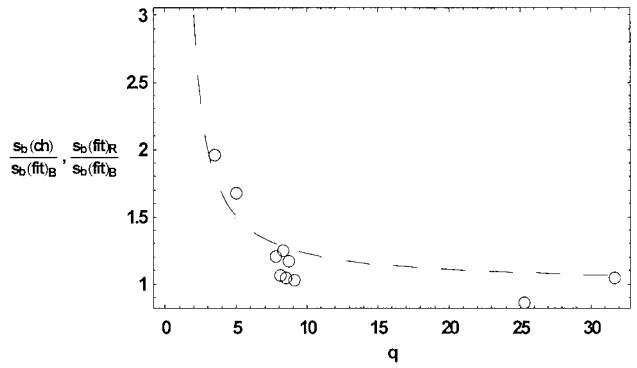

Figure 6. Comparison of $s_b(\text{ch})/s_b(\text{fit})_B$ (data points) and $s_b(\text{fit})_R/s_b(\text{fit})_B$ (dashed line), plotted against the number of arms q.

The q values given in Table 1, both theory and chemistry, agree very well except for PBC2 and PBC4 in which only moderate agreement is obtained. Increas-

ing the value of q produces its largest effect on the ratio of the two plateaus given by the arm and backbone contributions, as can be easily seen in the rheological response. The observed discrepancy in Table 1 between the q values obtained from theoretical modeling and chemistry remains to be explained.

The theory outlined above can be seen to be extremely accurate in capturing the linear rheological response of varied comb polymers. However, due to the exponential factors appearing in the expressions for the relaxation times, it is a little difficult to predict the linear viscoelastic response of any particular comb polymer ahead of time. Taking PBC6, for example, an increase of 10% in its arm molecular weight would lead to its terminal time being increased by roughly a factor of 3.

As mentioned in the Introduction, the method of attachment of arms to the cross-bar[14] yields a Poisson distribution in the number of attached arms. Taking this distribution into account fully would be straightforward but lengthy in detail, so here we estimate the degree of approximation expected using our monodisperse q assumption. The principal effect of the distribution in the number of arms, via the variance $\sim 1/\sqrt{q}$, in the number of arms $\sim q$, is to broaden the terminal time. The variance $\sim 1/\sqrt{q}$ can be seen to be small for most the comb polymers studied (e.g., for PBC 6 $1/\sqrt{q} \sim 1/3$). PBC3 and PBC8, on the other hand, possess a relatively low number of arms, and we do indeed observe a more broadened reptation peak than theory predicts.

We find above for comb polymers two distinct and discernible regimes for the low-frequency relaxations. If the number of arms distributed along the cross-bar is relatively small (Figure 1), then we find that the comb cross-bar behaves as essentially a H-polymer cross-bar.[6] On the other hand, if the number of arms along the comb cross-bar is relatively large (Figure 2), then we find the low-frequency relaxations to be drastically altered, and the linear rheological response of comb polymers will differ markedly from that of H-polymers. We can resolve this separation of low and high q dynamical regimes quantitatively as follows for comb polymers. The criterion for using the high q, distributed drag treatment above is that the portion of backbone relaxed by fluctuations, cutoff at the reptation time, should contain more than one branch point. Quantitatively, this criterion reads $s_{rep} = 1/(M_b/2M_e^*)^{1/2} > 2/q$ or $q_{crit} > (2M_b/M_e^*)^{1/2}$, where M_e^* takes into account the "effective" entanglement molecular weight due to the fraction of already relaxed material. For example, using the above criterion for PBC8 which has $\phi_b \sim 1/2$ and $q = 3$ arms, we find $q_{crit} = 10$ and therefore $q < q_{crit}$, and we must have the low q relaxation dynamics dominated by the local frictional drag at the chain ends as in the H-polymer case. However, using the above criterion for PBC7 which has $\phi_b \sim 1/4$ and $q = 8$ arms, we find $q_{crit} = 5$ and therefore $q > q_{crit}$, and we must have the high q relaxation dynamics dominated by the distributed frictional drag along the comb cross-bar.

In Figure 3 we can see the effect of arm length on the rheology. Increasing the arm length leads to a broadening of the rheological spectra at intermediate frequencies, as well as providing more arm material to undergo starlike activated diffusion behavior. In Figure 4 we can see the effect of backbone length on the rheology. Increasing the backbone length leads to a larger terminal time, as well as providing a higher concentration of backbone material to undergo late-time reptative behavior.

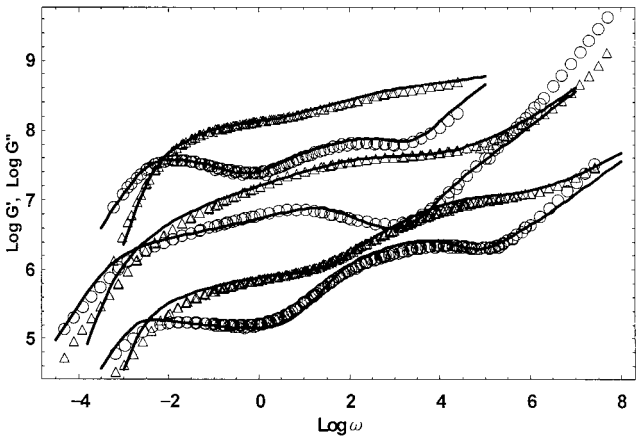

Figure 7. Comparison of experimental data and theoretical predictions for $G'(\omega)$ and $G''(\omega)$ for (from bottom to top) a comb polymer PBC6, a star polymer S105, and a H-polymer H110B20A. S105 and H110B20A have been shifted vertically by a factor of 100 and 1000, respectively.

We are now in a position to discuss the different response of star, H, and comb architectures. Shown in Figure 7 is a comparison of experimental data and theoretical predictions for $G'(\omega)$ and $G''(\omega)$ for a comb polymer PBC6, a polyisoprene star polymer S105 with arm length 105 kDa,[24] and a polyisoprene H-polymer H110B20A with a backbone length of 110 kDa and arm length 20 kDa.[6] The two universal (for PI) parameters G_0 and τ_e were taken to be 0.52 MPa and 7×10^{-6} s at 25 °C.[21] Values used for M_e were around 4500 g mol^{-1} for PI.[21]

From the figure we can clearly observe the dramatic effects of topology on polymer dynamics. For a typical star polymer we see a very broad maximum in its rheological spectrum, which is due to the exponential dependence of the arm relaxation time on the arm molecular weight and spread of spatially localized relaxation modes along the arm. The low-frequency reptative peak associated with any backbone material present is absent for stars. For comb and H-polymers we again see starlike behavior at intermediate frequencies due to the relaxation of arm material, eventually giving way at low frequencies to reptative motion of the backbone. The difference between the backbone dynamics of comb and H-polymers can be clearly seen in Figure 7. For H-polymers we see a much more sharply defined reptation peak than for comb polymers. This is rather typical of combs for two reasons. First, it is consistent with the much greater number of relaxation modes available to backbones of comb polymers, where the frictional drag is distributed along the backbone, over that of H-polymers where the frictional drag is localized at the backbone extremities, leading to the existence of only one single path length fluctuation mode. Second, a higher number of arms tends to dilute the cross-bar fraction relative to an H-polymer with the same arm and cross-bar molecular weights. It is worth pointing out that a "pom-pom" architecture would contain the second, dilution, effect but not the first.

5. Conclusion

We have studied the dynamics of entangled comb polymers in linear rheological response.

The rheology is well accounted for by the assumption of path length retraction in any dangling arms present, followed by reptation/fluctuation of the cross-bar present. For comb polymers (as for H-polymers[6]), the presence of the cross-bar has several important consequences for the relaxation of the dangling arms. First, their presence as unrelaxed material during the faster dynamics of the arms greatly slows down the arm retraction relative to the rate it would adopt in a melt of pure stars. The coefficient of M_a/M_e in the exponential term for all long time scales increases with the fraction of cross-bar material. Second, the presence of this effectively fixed network fraction enhances the role of polydispersity in the arm molecular weight. The presence of even the small degree of polydispersity arising in anionic polymerizations shifts the terminal time of the retracting arms to a longer time scale than would result from a monodisperse ensemble possessing the same weight-average molecular weight.

The rheology is also well accounted for by careful consideration of the effect of the number of arms a comb polymer has distributed along its backbone. The rheology shows that if a comb polymer possesses a small number of arms, then we can essentially consider its backbone dynamics as comprising a set of independent relaxation modes, like a H or pom-pom polymer. However, if the number of arms increases, then we get coupled frictional blob dynamics along the comb backbone. This signature can be clearly seen in the linear rheological response of our model comb polymers. We do not see any sign of the anomalously rapid relaxation reported for similar polyisoprene architectures in ref 13, nor of anomalously slow branch point motion reported in asymmetric stars,[12] despite the wide variety of architectures explored.

We emphasize that the approach given here is completely generic for combs. A satisfactory theory for the linear response of these topologically complex polymers is a requirement for any understanding of their nonlinear response. In particular, the stress in transient extension for combs is expected to exhibit strong "hardening" under large strains and strain rates. A study of these materials in strong flows will be the subject of a future report.[25] Finally, comb polymers take us a step closer to the rheology of industrial polymers than canonical pom-pom[26] polymers. This is due not only to the presence of (Poisson) polydispersity in arm number but also to the direct relevance of the comb structure. In one case at least (metallocene single-site branched resins), the low-frequency topology of the molecules is predominantly comblike when branching frequency is high.[27]

Acknowledgment. This work was funded by the European Community under the Industrial & Materials Technologies Programme (Brite-Euram) Contract BRPR-CT97-0599 and Project BR-97-4248.

References and Notes

(1) Doi, M.; Edwards, S. F. *The Theory of Polymer Dynamics*; Oxford University Press: New York, 1986.
(2) Osaki, K.; Kurata, M. *Macromolecules* **1980**, *13*, 671.
(3) Rubinstein, M. *Phys. Rev. Lett.* **1987**, *59*, 1946. Deutsch, J. M.; Madden, T. L. *J. Chem. Phys.* **1989**, *91*, 3252. O'Connor, N. P. T.; Ball, R. C. *Macromolecules* **1992**, *25*, 5677.
(4) Fetters, L. J.; Kiss, A. D.; Pearson, D. S.; Quack, G. F.; Vitus, F. J. *Macromolecules* **1993**, *26*, 647.
(5) Milner, S. T.; McLeish, T. C. B. *Macromolecules* **1997**, *30*, 2159.
(6) Mcleish, T. C. B.; et al. *Macromolecules* **1999**, *32*, 6734.
(7) Roovers, J. *Macromolecules* **1984**, *17*, 1196. Roovers, J.; Toporwski, P. M. *Macromolecules* **1987**, *20*, 2300.
(8) Roovers, J.; Graessley W. W. *Macromolecules* **1981**, *14*, 766.
(9) McLeish, T. C. B. *Phys. World* **1995**, *8*, 32.
(10) McLeish, T. C. B. In *Theoretical Challenges in the Dynamics of Complex Fluids*; McLeish, T. C. B., Ed.; Kluwer: Dordrecht, 1997.
(11) Yurasova, T. A.; Mcleish, T. C. B.; Semenov, A. N. *Macromolecules* **1994**, *27*, 7205.
(12) Frischknecht et al., submitted to *Macromolecules*.
(13) Archer et al., submitted to *Macromolecules*.
(14) Fernyhough, C. M.; Young, R. N. The Synthesis and Characterization of Polybutadiene and Poly(ethylene-1-butene) Combs. *Macromolecules* **2001**, *34*, 7034.
(15) Milner, S. T.; McLeish, T. C. B.; Johnson, J.; Hakiki, A.; Young, R. N. *Macromolecules* **1998,** *31*, 9345.
(16) Likhtman, A., personal communication.
(17) Doi, M.; Kuzuu, N. Y. *J. Polym. Sci., Polym. Lett. Ed.* **1980**, *18*, 775. Pearson, D. S.; Helfand, E. *Macromolecules* **1984**, *19*, 888. Ball, R. C.; McLeish, T. C. B. *Macromolecules* **1989**, *22*, 1911.
(18) Ball, R. C.; McLeish, T. C. B. *Macromolecules* **1990**, *22*, 1911.
(19) Frischknecht et al. *Macromolecules* **2000**, *33*, 9764.
(20) Milner, S. T.; McLeish, T. C. B. *Phys. Rev. Lett.* **1998,** *81*, 725.
(21) Ferry, J. D. *Viscoelastic Properties of Polymers*; Wiley: New York, 1980.
(22) Struglinski et al. *Macromolecules* **1985**, *18*, 2680.
(23) Fetters et al. *J. Polym. Sci., Part B: Polym. Phys.* **1999**, *37*, 1023.
(24) Daniels, D. R.; et al. *Rheol. Acta*, in press.
(25) Daniels, D. R.; McLeish, T. C. B.; Crosby, B. J.; Young, R. N.; Fernyhough, C. M.; Larson, R. G. Molecular Rheology of Comb Polymer Melts II: Nonlinear Response, in preparation.
(26) McLeish, T. C. B.; Larson, R. G. *J. Rheol.* **1998**, *42*, 81.
(27) Read, D. J.; Mcleish, T. C. B. *Macromolecules* **2001**, *34*, 1928.

MA010712P